

Spacer Control the Dynamic of Triplex Formation between Oligonucleotide-Modified Gold Nanoparticles

Honglian Yan,^{†,§} Cen Xiong,^{†,§} Hong Yuan,[‡] Zunxiang Zeng,[†] and Liansheng Ling^{*,†}

State Key Laboratory of Optoelectronic Materials and Technologies, School of Chemistry and Chemical Engineering, Sun Yat-Sen University, Guangzhou 510275, and College of Science, State Key Laboratory of Agricultural Microbiology, Huazhong Agricultural University, Wuhan 430070, People's Republic of China

Received: June 9, 2009; Revised Manuscript Received: August 14, 2009

A novel method was developed to control the dynamic of triplex formation between oligonucleotide-modified gold nanoparticles in the presence of complementary strand. The solution containing the oligonucleotide 5'-SH-ACA CAC ACA CAC CTT TCT TTC CTT TCT TTC-3'(oligo-1)-modified gold nanoparticles was red in color. Due to triplex formation, there was a tiny change in color on addition of the complementary oligonucleotide 5'-GAA AGA AAG GAA AGA AAG-3'(oligo-3). The addition of oligonucleotide 5'-GTG TGT GTG TGT-3'(oligo-2) induced the spacer portion of oligo-1 to change from single strand to rigid duplex structure and protrude from the surface of the gold colloid, removing the physisorption between oligo-1 and the gold nanoparticles successfully. Therefore, when the oligo-2 was added accompanied by oligo-3 at pH 5.6 and 6.0 μM spermine, larger aggregates were formed and the color of the solution changed from red to blue within 20 min. The oligo-2 hybridized with the spacer portion of oligo-1 and had no effect on the stability of triplex DNA; thereby, the melting temperatures of the triplex DNA were 51 and 53 °C in the absence and presence of oligo-2, respectively. Oligo-3 played a crucial role in the triplex formation between nanoparticles. When oligo-3 was replaced with 5'-GAA AGA AAG TAA AGA AAG-3' (oligo-4, single-base mismatched) and 5'-GAA AGT AAG GAA TGA AAG-3' (oligo-5, double-base mismatched), respectively, the melting temperature decreased from 53 to 41 °C and eventually to 33 °C.

Introduction

Oligonucleotides generally bind to the major groove of the double-stranded DNA (ds-DNA) by forming triplex DNA. Such triplex formation plays a crucial role in the process of gene translation,¹ DNA transcription, replication, and cleavage.^{2–4} Therefore, it is important and beneficial to develop a new method to investigate triplex DNA. Methods presently reported to be in use are based upon fluorescent probes,⁵ atomic force microscopy,^{6–8} EPR, and CD (circular dichroism).⁹

Lately, gold nanoparticles (AuNPs) have been widely studied in developing biosensors because of their special optical characteristics.^{10,11} Many useful biosensors based upon DNA hybridization,^{12–14} PCR,^{15,16} conformation change between ds-DNA and tetraplex DNA,^{17–19} gene knockout,²⁰ DNA–protein interaction,^{21,22} and interaction between DNA and molecules have been reported.^{23,24} Triplex DNA contains the Watson–Crick bond and the Hoogsteen bond. The latter bond is weaker than the former,⁷ and thus the environment easily influences the formation of triplex DNA. The physisorption of DNA and gold colloid surface is unfavorable for triplex formation between oligonucleotide-modified AuNPs. Therefore, for formation of triplex this physisorption must be overcome. One method is to increase the stability of triplex DNA by adding a triplex binding molecule,^{25,26} keeping the solution in refrigerated at 4 °C²⁷ or by backbone modifications such as locked nucleic acids (LNAs) for instance.²⁸ Another method is to keep the solution at 90 °C

for 5 min and then to slowly cool it down to room temperature to reduce the effect of electrostatic interaction.²⁹ Here, we report the triplex formation between oligonucleotide-modified AuNPs that depends partly on the complementary strand for spacer.

Experimental Section

Materials. HAuCl₄·3H₂O was purchased from Sigma-Aldrich Co. Au atomic absorption standard solution GSB G62068-90 (National Analysis Center for Iron and steel, China) was used for calibration. Spermine ($\text{H}_2\text{N}(\text{CH}_2)_3\text{NH}(\text{CH}_2)_4\text{NH}(\text{CH}_2)_3\text{NH}_2$) was obtained from Sigma-Aldrich Co. Unless stated otherwise, all the chemicals were of analytical reagent grade or better. Nanopure water (18.1 MΩ) was obtained from a 350 Nanopure water system (Guangzhou Crystalline Residue Desalination of Sea Water and Treatment Co. Ltd.) and used for all experiments. Bis-tris buffers of pH values 7.0 and 5.6 (both 50 mM NaCl), and acetate buffer of pH value 5.0 (50 mM NaCl) were used in our experiments. Ru(bipy)₂dppx²⁺ (bipy = 2,2'-bipyridine, dppx = 7,8-dimethyl-dipyridophenazine) was prepared by us.

Apparatus. A TU-1901 UV–visible absorption spectrometer (Beijing Pukinje General Instrument CO., Ltd) was used to obtain the absorption spectrum. A high-speed Anke GL-20G-Π centrifuge (Anting Scientific Instrument Factory, Shanghai, China) was utilized to centrifuge the mixture of DNA and Au nanoparticles. Transmission electron microscope (TEM) images were recorded with a JEM-2010HR transmission electron microscope (Japan). Luminescence was detected with an RF-5301 (Shimadzu, Japan) spectrofluorometer equipped with a quartz cell (1 × 1 cm² cross-section).

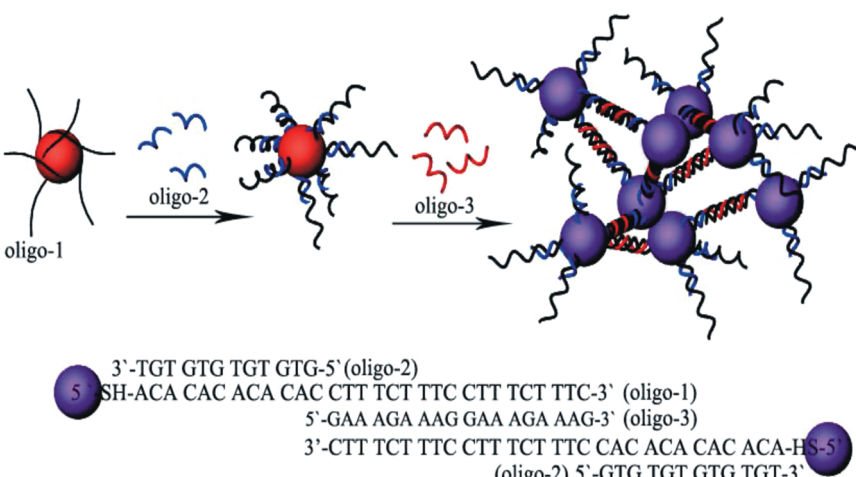
Measurement of Melting Temperature. Temperatures were measured with a TU-1901 UV–visible absorption spectrometer to draw up the melting curve.

* To whom correspondence should be addressed. Tel: 0086-20-84110156.
E-mail: cesllsh@mail.sysu.edu.cn.

[†] Sun Yat-Sen University.

[‡] Huazhong Agricultural University.

[§] These authors contributed equally to this work.

SCHEME 1: Assembly of DNA-Modified AuNPs Promoted by the Formation of Triplex DNA

Design of Oligonucleotides. Oligonucleotides with a length of 30 bases were selected. Within this ss-DNA, 18 homopyrimidine bases were used for triplex formation. The additional 12 bases acted as spacers between that portion of triplex formation and the surfaces. To bind the ss-DNA covalently to the gold surfaces, mercapto-modified oligodeoxyribonucleotide with a sequence of 5'-SH-ACA CAC ACA CAC CTT TCT TTC CTT TCT TCT TTC-3'(oligo-1) was used. As shown in Scheme 1, an oligonucleotide with a sequence of 5'-GTG TGT GTG TGT-3' (oligo-2) was used to form dsDNA with the spacer portion of oligo-1, which caused the oligo-1 protrude from the gold surface and overcome the physisorption. Oligonucleotide with a sequence of 5'-GAA AGA AAG GAA AGA AAG-3' (oligo-3) was used to form dsDNA with homopyrimidine bases of oligo-1, and the dsDNA(oligo-1 and oligo-3) from one nanoparticle combined with oligo-1 from another nanoparticle to form triple helical structures. Oligonucleotides with a sequence of 5'-GAA AGA AAG TAA AGA AAG-3'(oligo-4) and 5'-GAA AGT AAG GAA TGA AAG-3' (oligo-5) are single-base- and double-base-mismatched for triplex formation, respectively. Oligonucleotide 5'-GTG TGT ATG TGT-3'(oligo-6) is single-base-mismatched for the spacer portion.

Deprotection of Thiol-Modified Oligonucleotide. The disulfide bond at the bottom of the oligo-1 was reduced by tri-(2-carboxyethyl) phosphine (TCEP), which is active in acid solution except with PBS buffer. 5OD oligodeoxyribonucleotide powder was dissolved in 20 μ L of acetate buffer (pH 5.0, 10 mM), and 2.0 μ L of TCEP (20 mM) was added and kept for 1.0 h to sever the disulfide bond.³⁰

Preparation of Gold Nanoparticles. Au nanoparticles were prepared by reducing HAuCl₄ with citrate.³¹ The sizes of the nanoparticles and their distribution were obtained by measuring at least 200 particles from TEM images. The Au nanoparticles prepared for this study were 14.2 ± 1.2 nm in diameter. The density of the spherical nanoparticles was equivalent to that of bulk gold (19.30 g/cm^3), and the average nanoparticle mass was calculated ($M = 1.7 \times 10^7\text{ g/mol}$). The atomic gold concentration in the solution of Au nanoparticles was determined by inductively coupled plasmon atomic emission spectroscopy (Spectro Ciros Vision Eop, Germany). Comparing of atomic gold concentration in the particle solution to the average nanoparticle mass which obtained from the TEM analysis, the molar concentration of gold nanoparticles in a given preparation was 10.45 nM. By measuring the UV-vis absorption of nanoparticles solutions at 522, extinction coefficient (ϵ at 522 nm) of the nanoparticles was calculated ($2.6 \times 10^8\text{ M}^{-1}\text{ cm}^{-1}$).

Preparation of Oligonucleotide-Modified Nanoparticles. 5'-SH-(CH₂)₆-modified oligonucleotides (5OD, 22.0 μ L) were treated with TCEP before being added to a 10 mL solution of Au nanoparticles (10.45 nM), which was stored at 25 °C for 18 h. NaCl solution was then added (the final concentration is 0.1 M) to it and allowed to incubate for another 44 h. Excess reagents were then removed by centrifugation at 15 000 rpm for 20 min. Following removal of the supernatant, the red oily precipitate that remained contained the DNA-modified Au nanoparticles, which were collected for our experiments. All experiments were carried out at room temperature (22 °C).

Coverage of Oligonucleotide on the Nanoparticles. The surface coverage of gold nanoparticles was measured by a nucleic acid “light-switch” molecule, Ru(bipy)₂(dppx)²⁺, which emits strong luminescence when intercalated into the duplex DNA, even when it is quenched completely by water in an aqueous solution.³² The oligodeoxyribonucleotides on the nanoparticle surfaces were displaced overnight with 0.1 M DTT at room temperature followed by the separated oligonucleotides from the nanoparticles by centrifugation. The supernatant was diluted to 3.0 mL with 50 mM NaCl, 10 mM PBS (pH 7.0) containing 1.0 μ M Ru(bipy)₂(dppx)²⁺. Luminescence intensity was determined after adding enough complementary strands (oligo-3) of the target sequence, after which the DNA concentration was calculated from the working curve. The excitation and emission wavelengths were 467 and 613 nm. The number of oligonucleotides per gold nanoparticle was calculated by dividing the concentration of duplex oligonucleotide by the concentration of nanoparticles. For this experiment, the average coverage of oligonucleotides on the nanoparticle was found to be 30 ± 2.3 strands per nanoparticle.

Hybridization Percentage of the Spacer. The samples containing 3.5 nM oligo-1-modified Au nanoparticles and 500 nM oligo-2 were held at 4 °C for 12 h to allow them to hybridize adequately. The nonhybridized oligo-2 was removed by rinsing and centrifuging twice with PBS buffer solution. After this, 1.0 M DTT was used to displace the oligo-1 on the gold nanoparticle surface, and the displaced oligonucleotides were separated from the nanoparticles by centrifugation. The supernatant was diluted to 3.0 mL with 50 mM NaCl and 10 mM PBS containing 1.0 μ M Ru(bipy)₂dppx²⁺. The luminescence was measured, and the concentration of dsDNA that formed prior to the process of removing from the nanoparticles calculated according to linear equations. Enough oligo-2 was then added to ensure that all oligo-1 was hybridized with oligo-2 and the total concentration of oligo-2 was calculated according to the luminescence

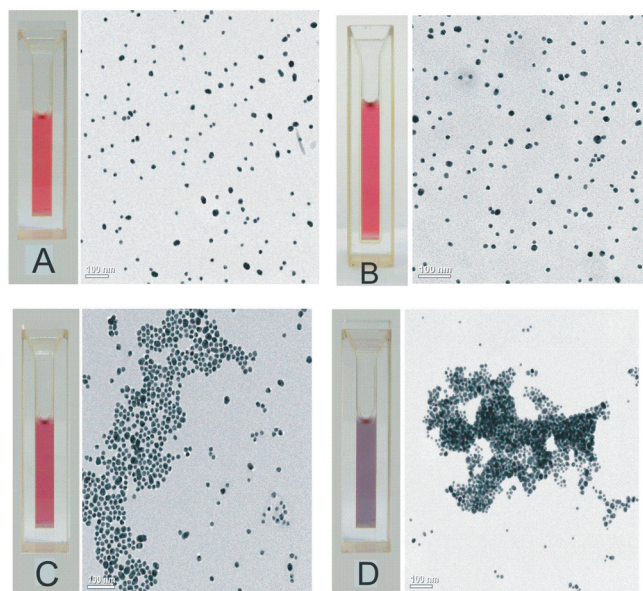


Figure 1. Color photo and TEM image of DNA–AuNPs composites at pH 5.6 (A) 3.5 nM AuNPs-oligo-1 + 6.0 μ M spermine. (B) A + 500 nM oligo-2. (C) A + 150 nM oligo-3. (D) A + 500 nM oligo-2 + 150 nM oligo-3.

intensity. Therefore, the hybridization percentage could be calculated with these two concentrations, and in this work was found to be about 12% for 3.5 nM oligo-1-modified Au nanoparticles.

Results and Discussion

Multivalent cations, such as spermine ($(\text{H}_2\text{N}(\text{CH}_2)_3\text{NH}(\text{CH}_2)_4\text{NH}(\text{CH}_2)_3\text{NH}_2$) and magnesium, are usually applied to neutralize the negative charge in the study of triplex DNA.³³ The charge of magnesium is 2+, while that of spermine is 4+; thus, spermine is a more effective charge neutralizer. Therefore, we selected spermine as the DNA charge neutralizer. While excess spermine can induce DNA condensation,³⁴ multivalent cations can induce the precipitation of Au nanoparticles as well.³⁵ When the nanoparticles are assembled with a layer of DNA, the ability of resisting multivalent cations increased. The maximum concentration of spermine was 12.0 μ mol/L after the nanoparticles were modified with oligo-1; the higher concentration of spermine resulted in the aggregation and precipitation of DNA modified nanoparticles, and so it was necessary to keep the spermine concentration lower than 12.0 μ mol/L. We found that concentration of 4.0 μ mol/L could induce the formation of triplex DNA; therefore, the concentration of spermine we used was within the range 4.0–12.0 μ mol/L. In our experiments, to ensure that triplex DNA forms at room temperature, 6.0 μ mol/L spermine was used as DNA charge neutralizer.

Attraction of electrostatic forces between the AuNPs and nucleotides caused the ss-DNA to adsorb onto the gold colloid,^{35–37} which might have affected the formation of triplex DNA between the nanoparticles. To investigate the effect of DNA conformation of the spacer portion, experiments were carried out with and without complementary strands (oligo-2). As shown in Figure 1B, no color change was observed only in the presence of oligo-2, an observation that tallies well with the results of TEM; however, there was a tiny change in the color of the solution in the presence of oligo-3 solely, and mild aggregation was observed in the TEM image (Figure 1C). However, the color of the solution changed dramatically from red to purple in the presence of oligo-2 and oligo-3, and large

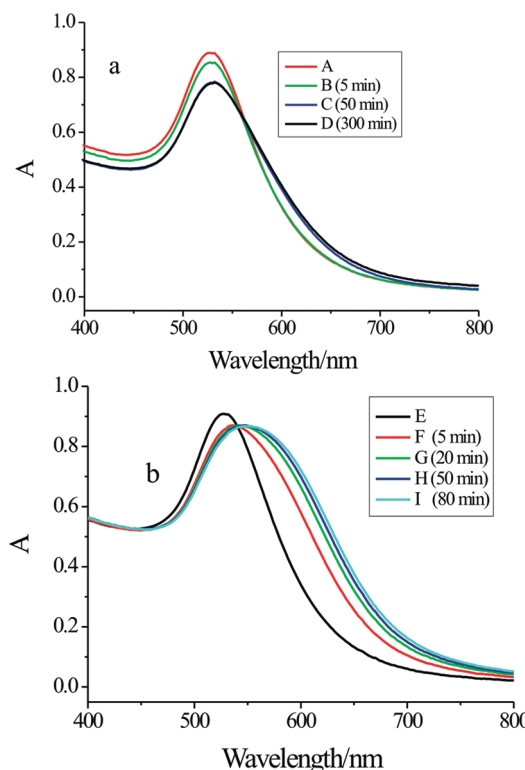


Figure 2. Absorption spectrum of DNA–Au nanoparticles composites at different time under pH 5.6 in the presence of 6.0 μ M spermine with and without oligo-2. (A) 3.5 nM AuNPs-oligo-1 ($\lambda_{\text{max}} = 526$ nm). (B) A + 150 nM oligo-3 (5 min, $\lambda_{\text{max}} = 532$ nm). (C) A + 150 nM oligo-3 (50 min, $\lambda_{\text{max}} = 532$ nm). (D) A + 150 nM oligo-3 (300 min, $\lambda_{\text{max}} = 532$ nm). (E) 3.5 nM AuNPs-oligo-1 + 500 nM oligo-2 ($\lambda_{\text{max}} = 526$ nm). (F) E + 150 nM oligo-3 (5 min, $\lambda_{\text{max}} = 536$ nm). (G) E + 150 nM oligo-3 (20 min, $\lambda_{\text{max}} = 542$ nm). (H) E + 150 nM oligo-3 (50 min, $\lambda_{\text{max}} = 548$ nm). (I) E + 150 nM oligo-3 (80 min, $\lambda_{\text{max}} = 550$ nm).

aggregation was observed in the TEM image (Figure 1D). The hybridization of oligo-2 with the spacer portion of oligo-1 resulted in the conformation change from coiled ssDNA to rigid dsDNA, which caused the oligo-1 to protrude and desorb away from the nanoparticle surface, thus helping to overcome the physisorption between oligo-1 and gold colloid surface. Therefore, the addition of oligo-2 favored the formation of triplex between nanoparticles and the assembly process of oligonucleotide-modified nanoparticles.

To further study the effect of oligo-2, the absorption spectra of samples were collected at different time intervals. As shown in Figure 2a, absorption spectra of the sample without oligo-2 were collected at intervals of 0, 5, 50, and 300 min, respectively. The maximum wavelength of the sample red-shift from 526 to 532 nm occurred within 5 min, but it did not change further with lapse of time to 300 min; only the absorption intensity reduced weakly. These changes may have occurred due to the physisorption between ssDNA and the gold surface. For comparison, as shown in Figure 2b, the absorption spectra changed dramatically in the presence of oligo-2 and oligo-3, and the maximum wavelength red-shift from 526 to 550 nm occurred within 80 min. These results reveal that the physisorption is controlled by the DNA conformation of spacer portion and that the rigid structure of dsDNA could overcome physisorption effectively, while the random structure of ssDNA could not. Therefore, it was important to keep the spacer with the dsDNA conformation to overcome the physisorption, as it was helpful in the formation of triplex DNA. According to this result, oligo-2 was added prior to each experiment.

Protonation of Cytosine (C) is essential for the formation of C⁺GC base triplets; thus, the stability of triplex DNA containing C⁺GC triplets depends on the pH value. Therefore, experiments were carried out at pH values of 5.0, 5.6, and 7.0, respectively. The color of the solution changed from red to blue at a pH value of 5.0 within 20 min in the presence of oligo-2 and oligo-3, and the maximum wavelength red shift from 526 to 558 nm (see Supporting Information). The color changed from red to purple at a pH value of 5.6 in the presence of oligo-2 and oligo-3 as well and the maximum wavelength red-shift from 526 to 544 nm. However, these results could not be obtained at pH value 7.0, and the solution color remained red in the presence of oligo-2 and oligo-3, and there were also no changes observed in the absorption spectrum. These results revealed that triplex formation occurred between nanoparticles at pH values of 5.0 and 5.6, and simultaneously promoted the assembly of nanoparticles and changes in the surface plasma resonance absorption band. However, the assembly was irreversible at pH value 5.0, hence pH value 5.0 was not suitable. Therefore, pH 5.6 was selected for our experiments.

The formation of parallel triplex is based upon the formation of C⁺GC and TAT base triplets. Therefore, mismatches could affect the stability of triplex DNA. In order to study the possibility of applying this method to DNA recognition, experiments involving complementary strands, single-base mismatched strands, and double-base mismatched strands were carried out. As shown in Figure 3a, the color of the solution changes from red to purple after the addition of the complementary strand (oligo-3), while the color changes do not manifest when single-base mismatched strand (oligo-4) and double-base mismatched strand are added separately. These results revealed that DNA mismatch attenuates the stability of triplex DNA dramatically, and this method could be used to identify oligonucleotides with homopyrimidine strands. The addition of single-base mismatched strand (oligo-6) for the spacer portion of oligo-1 had little effect on triplex formation, and the color of the solution (Figure 3b) was different from that of the complementary strand (oligo-2). Thus, this phenomenon could be used to identify nonhomopyrimidine strands with the spacer portion of oligo-1 as well.

To further investigate the effect of base mismatch on the stability of triplex DNA, melting curves that contained complementary strands (oligo-3), single-base mismatched strands (oligo-4) and double-base mismatched strands were carried out, respectively. It was shown in Figure 4a that triplex DNA has two melting temperatures in the absence of nanoparticles and in the presence of oligo-3: the first at 26 °C unbinds the Hoogsteen bond, and the second at 52 °C unbinds the Watson–Crick bond. The respective individual melting temperatures in the presence of oligo-4 were found to be 17 and 48 °C. Only one melting temperature at 46 °C was observed in the presence of oligo-5. In the above-mentioned method, the melting process of Hoogsteen bond was weaker and could be easily enshrouded by the melting process of Watson–Crick bond, which was in good agreement with the report that Watson–Crick bond is stronger than that of Hoogsteen bond.⁷ For comparison, melting curves for triplex DNA that were formed between oligo-modified nanoparticles are reproduced in Figure 4b; only one melting transition is observed in the presence of oligo-3. The Hoogsteen bond being weaker than the Watson–Crick bond,⁷ it unbound more easily than the latter; thus, the melting curve represents the unbinding process of the Hoogsteen bond in triplex DNA. The melting temperature in the presence of complementary strand (oligo-3) was 53 °C.

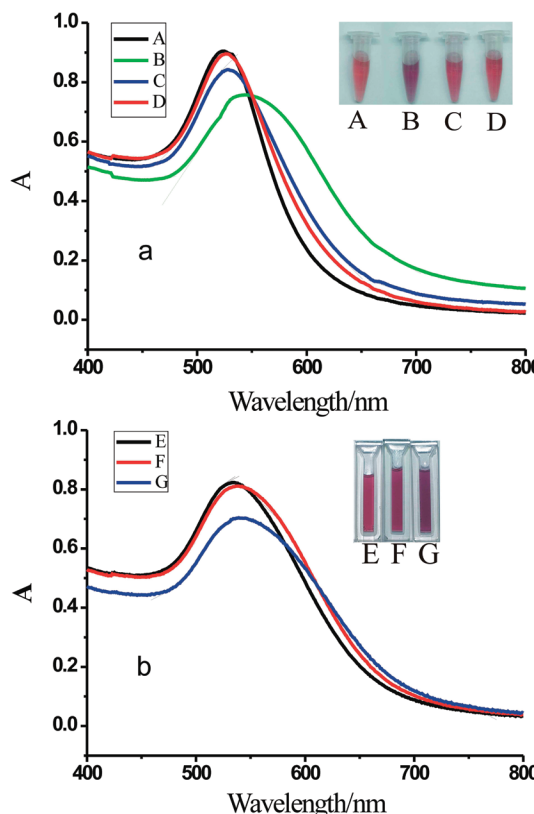


Figure 3. Color photos and absorption spectrum of DNA–Au nanoparticle composites after adding different oligos under pH 5.6 at room temperature (22 °C). (A) 3.5 nM AuNPs-oligo-1 + 6.0 μM spermine + 500 nM oligo-2. (B) A + 150 nM oligo-3 (complementary strand). (C) A + 150 nM oligo-4 (single-base mismatched strand). (D) A + 150 nM oligo-5 (double-base mismatched strand). (E) 3.5 nM AuNPs-oligo-1 + 6.0 μM spermine + 150 nM oligo-3. (F) E + 500 nM oligo-6 (one base mismatch for spacer part of oligo-1). (G) E + 500 nM oligo-2 (complementary strand for spacer part of oligo-1).

However, it was 41 and 33 °C, respectively, for single-base mismatched strand (oligo-4) and double-base mismatched strand (oligo-5). These results revealed that modifying DNA in the AuNPs noticeably increased the stability of complementary triplex DNA compared with triplex DNA that had no nanoparticles, and that the stability of triplex DNA dwindled dramatically when the strand contained a mismatched base. Individual melting temperatures for triplex DNA were found to be 51 and 53 °C in the absence and presence of oligo-2 (see Supporting Information), respectively, and revealed that the addition of oligo-2 had little effect on the stability of triplex DNA. This was in good agreement with the ref 34.

There are two obstacles to be overcome for triplex formation between oligonucleotide modified AuNPs. The first is the electrostatic repulsion between oligonucleotide modified nanoparticles. The second is the physisorption between ssDNA (or bases) and Au surface, which obstructs triplex formation as well. Two methods were used to solve the difficulties. Firstly, we overcame electrostatic repulsion with the addition of spermine, which has a molecule with a positive charge of four and is an effective charge neutralizer. Secondly, we eliminated physisorption by changing the DNA conformation near the surface. As dsDNA has a rigid structure, there is no physisorption between dsDNA and gold surface; this physisorption disappears as soon as the spacer hybridizes with its complementary strand (oligo-2).^{39,40} Therefore, the complementary strand (oligo-2) for the spacer

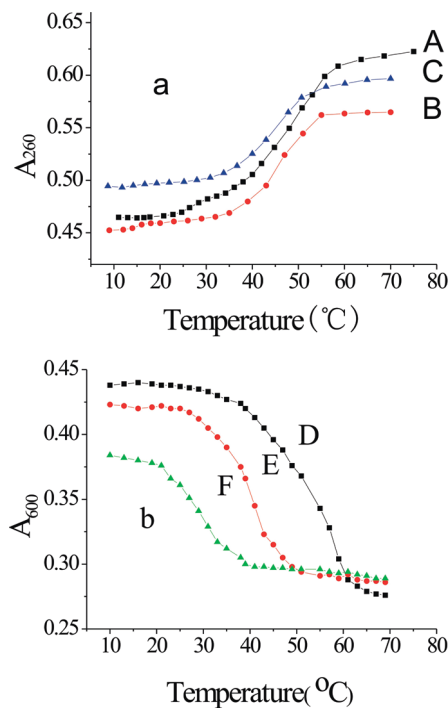


Figure 4. Melting curves of triplex DNA without (a) and involving (b) nanoparticles in the presence of complementary, single-base mismatch and two-base mismatch oligos. (A) 1.34 μ M oligo-1 + 0.45 mM spermine + 0.66 μ M oligo-2. (B) 1.34 μ M oligo-1 + 0.45 mM spermine + 0.66 μ M oligo-4 (C) 1.34 μ M oligo-1 + 0.45 mM spermine + 0.66 μ M oligo-5. (D) 3.5 nM AuNPs-oligo-1 + 6.0 μ M spermine + 500 nM oligo-2 + 150 nM oligo-3. (E) 3.5 nM AuNPs-oligo-1 + 6.0 μ M spermine + 500 nM oligo-2 + 150 nM oligo-4. (F) 3.5 nM AuNPs-oligo-1 + 6.0 μ M spermine + 500 nM oligo-2 + 150 nM oligo-5.

was used to overcome the physisorption. Although triplex formation dynamic is almost completely controlled by the conformation of spacer and this formation is easily observed when the conformation of spacer maintains the dsDNA structure at room temperature, the stability of triplex DNA is wholly not influenced only by the existence of complementary strand (oligo-2) for spacer. Consequently, the presence of oligo-2 does not change the properties of triplex DNA or its interaction with other molecules but only accelerates the formation of triplex–nanoparticle conjugates. Those enable the possible use of this method to remove physisorption between DNA bases and gold surfaces in other triplex-related research in the future. Therefore, triplex–AuNP conjugates form rapidly and the color of the solution changes from red to blue within a few minutes after addition of oligo-2 accompanied by oligo-3, and this process can be applied to sequence-specific identification of DNA at room temperature.

Conclusions

In brief, we developed a new method to overcome the physisorption between DNA bases and AuNPs in the formation of triplex. The color of the solution changed gradually because of the physisorption in presence of oligo-3 solely. For comparison, the rigid duplex structure formed at the spacer part of oligo-1 in the presence of oligo-2 and oligo-3, causing the oligo-1 protrudes from the surface of the AuNPs. Thus, triplex conjugates of AuNPs were formed within 20 min after the addition of oligo-3 together with

oligo-2. As a result, the color of the solution changed rapidly from red to purple. This color change can be used to sequence specifically recognize DNA at room temperature.

Acknowledgment. This work was supported by the Natural Science Foundation of China (No: 20645002) and SRF for ROCS, SEM.

Supporting Information Available: Effect of pH on the formation of triplex DNA–Au nanoparticles composites, Melting curve of triplex–AuNPs conjugates in the presence and absence of oligo-2. This material is available free of charge via the Internet at <http://pubs.acs.org>.

References and Notes

- (1) Knudsen, H.; Nielsen, P. E. *Nucleic Acids Res.* **1996**, *24*, 494–500.
- (2) Vasquez, K. M.; Narayanan, L.; Glazer, P. M. *Science* **2000**, *290*, 530–533.
- (3) Maine, I. P.; Kodadek, T. *Biochem. Biophys. Res. Commun.* **1994**, *204*, 1119–1124.
- (4) Radhakrishnan, I. R.; Patel, D. J. *J. Am. Chem. Soc.* **1993**, *115*, 1615–1617.
- (5) Mergny, J. L.; Garestier, T.; Rougee, M.; Lebedev, A. V.; Chassignol, M.; Thuong, N. T.; Helene, C. *Biochemistry* **1994**, *33*, 15321–15328.
- (6) Chemy, D. I.; Fourcade, A.; Svinarchuk, F.; Nielsen, P. E.; Malvy, C.; Delain, E. *Biophys. J.* **1998**, *74*, 1015–1023.
- (7) Ling, L. S.; Butt, H. J.; Berger, R. *J. Am. Chem. Soc.* **2004**, *126*, 13992–13997.
- (8) Ling, L. S.; Butt, H. J.; Berger, R. *Appl. Phys. Lett.* **2006**, *89*, 113902.
- (9) Gannett, P. M.; Darian, E.; Powell, J.; Johnson, I. L. E. M.; Mundoma, C.; Greenbaum, N. L.; Ramsey, C. M.; Dalal, N. S.; Budil, D. E. *Nucleic Acids Res.* **2002**, *30*, 5328–5337.
- (10) Mirkin, C. A.; Letsinger, R. L.; Mucic, R. C.; Storhoff, J. J. *Nature* **1996**, *382*, 607–609.
- (11) Rosi, N. L.; Mirkin, C. A. *Chem. Rev.* **2005**, *105*, 1547–1562.
- (12) Elghanian, R.; Storhoff, J. J.; Mucic, R. C.; Letsinger, R. L.; Mirkin, C. A. *Science* **1997**, *277*, 1078–1080.
- (13) Hazarika, P.; Ceyhan, B.; Niemeyer, C. M. *Angew. Chem., Int. Ed.* **2004**, *43*, 6469–6471.
- (14) Beissenhirtz, M. K.; Elnathan, R.; Weizmann, Y.; Willner, I. *Small* **2007**, *3*, 375–379.
- (15) Kim, E. Y.; Stanton, J.; Vega, R. A.; Kunstman, K. J.; Mirkin, C. A.; Wolinsky, S. M. *Nucleic Acids Res.* **2006**, *34*, e54.
- (16) Li, H.; Huang, J.; Lv, J.; An, H.; Zhang, X.; Zhang, Z.; Fan, C.; Hu, J. *Angew. Chem.* **2005**, *117*, 5230–5233.
- (17) Huang, C. C.; Huang, Y. F.; Cao, Z.; Tan, W.; Chang, H. T. *Anal. Chem.* **2005**, *77*, 5735–5741.
- (18) Liu, J.; Lu, Y. *Anal. Chem.* **2004**, *76*, 1627–1632.
- (19) Seela, F.; Jawalekar, A. M.; Chi, L.; Zhong, D. *Chem. Biodiv.* **2005**, *2*, 84–91.
- (20) Rosi, N. L.; Giljohann, D. A.; Thaxton, C. S.; Lytton-Jean, A. K. R.; Han, M. S.; Mirkin, C. A. *Science* **2006**, *312*, 1027–1030.
- (21) Hazarika, P.; Kukolka, F.; Niemeyer, C. M. *Angew. Chem., Int. Ed.* **2006**, *45*, 6827–6830.
- (22) Pavlov, V.; Xiao, Y.; Shlyahovsky, B.; Willner, I. *J. Am. Chem. Soc.* **2004**, *126*, 11768–11769.
- (23) Han, M. S.; Lytton-Jean, A. K. R.; Oh, B. K.; Heo, J.; Mirkin, C. A. *Angew. Chem., Int. Ed.* **2006**, *45*, 1807–1810.
- (24) Liu, J.; Lu, Y. *Angew. Chem., Int. Ed.* **2006**, *45*, 90–94.
- (25) Han, M. S.; Lytton-Jean, A. K. R.; Mirkin, C. A. *J. Am. Chem. Soc.* **2006**, *128*, 4954–4955.
- (26) Lytton-Jean, A. K. R.; Han, M. S.; Mirkin, C. A. *Anal. Chem.* **2007**, *79*, 6037–6041.
- (27) Jung, Y. H.; Lee, K. B.; Kim, Y. G.; Choi, I. S. *Angew. Chem., Int. Ed.* **2006**, *45*, 5960–5963.
- (28) McKenzie, F.; Faulds, K.; Graham, D. *Chem. Commun.* **2008**, *20*, 2367–2369.
- (29) Murphy, D.; Ritja1, R.; Redmond, G. *Nucleic Acids Res.* **2004**, *32*, e65.
- (30) Liu, J.; Lu, Y. *J. Am. Chem. Soc.* **2007**, *129*, 8634–8643.
- (31) Grabar, K. C.; Freeman, R. G.; Hommer, M. B.; Natan, K. J. *Anal. Chem.* **1995**, *67*, 735–737.
- (32) Ling, L. S.; He, Z. K.; Song, G. W.; Zeng, Y. E. *Anal. Chim. Acta* **2000**, *403* (1–2), 209–217.
- (33) Soyfer, V. N.; Potaman, V. N. *Triple Helical Nucleic Acids*; Springer: New York, 1996.

- (34) Bai, C.; Wang, C.; Xie, X. S.; Wolynes, P. G. *Proc. Natl. Acad. Sci.* **1999**, *96*, 11075–11076.
- (35) Ray, P. C. *Angew. Chem., Int. Ed.* **2006**, *45*, 1151–1154.
- (36) Maye, M. M.; Nykypanchuk, D.; Lelie, D. v. d.; Gang, O. *J. Am. Chem. Soc.* **2006**, *128*, 14020–14021.
- (37) Parak, W. J.; Pellegrino, T.; Micheel, C. M.; Gerion, D.; Williams, S. C.; Alivisatos, A. P. *Nano Lett.* **2003**, *3*, 33–36.
- (38) Storhoff, J. J.; Elghanian, R.; Mirkin, C. A.; Letsinger, R. L. *Langmuir* **2002**, *18*, 6666–6670.
- (39) Li, H. X.; Rothberg, L. *Proc. Natl. Acad. Sci.* **2004**, *101*, 14036–14039.
- (40) Xin, A. P.; Dong, Q. P.; Xiong, C.; Ling, L. S. *Chem. Commun.* **2009**, 1658–1660.

JP905408Q